Ecotoxicology and Environmental Safety 256 (2023) 114871

Contents lists available at ScienceDirect

Ecotoxicology and Environmental Safety

journal homepage: www.elsevier.com/locate/ecoenv

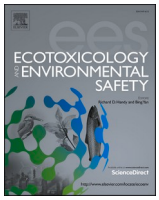

Tissue accumulation of polystyrene microplastics causes oxidative stress, hepatopancreatic injury and metabolome alterations in *Litopenaeus vannamei*

Yingxu Zeng [a,*], Baichuan Deng [b], Zixin Kang [a], Pedro Araujo [c], Svein Are Mjøs [d], Ruina Liu [a], Jianhui Lin [a], Tao Yang [a], Yuangao Qu [e]

[a] Key Laboratory for Coastal Marine Eco-Environment Process and Carbon Sink of Hainan Province, Yazhou Bay Innovation Institute, College of Ecology and Environment, Hainan Tropical Ocean University, Sanya 572000, China
[b] Guangdong Provincial Key Laboratory of Animal Nutrition Control, College of Animal Science, South China Agricultural University, Guangzhou 510642, China
[c] Institute of Marine Research, 5817 Bergen, Norway
[d] Department of Chemistry, University of Bergen, N-5020 Bergen, Norway
[e] Institute of Deep-Sea Science and Engineering, Chinese Academy of Sciences, Sanya 572000, China

ARTICLE INFO

Edited by Dr. G. Liu

Keywords:
Shrimp
Toxicity
Biomarkers
Metabolomics
Crustaceans

ABSTRACT

Microplastics (MPs) pose one of the major environmental threats to marine organisms and ecosystems on a global scale. Although many marine crustaceans are highly susceptible to MPs pollution, the toxicological effects and mechanisms of MPs on crustaceans are poorly understood. The current study focused on the impacts of MPs accumulation in shrimp *Litopenaeus vannamei* at the behavioral, histological and biochemical levels. The results demonstrated the accumulation of polystyrene MPs in various organs of *L. vannamei*, with highest MPs abundance in the hepatopancreas. The MPs accumulated in shrimp caused growth inhibition, abnormal swimming behavior and reduced swimming performance of *L. vannamei*. Following MPs exposure, oxidative stress and lipid peroxidation were also observed, which were strongly linked to attenuated swimming activity of *L. vannamei*. The above MPs-induced disruption in balance of antioxidant system triggered the hepatopancreatic damage in *L. vannamei*, which was exacerbated with increasing MPs concentrations (from 0.02 to 1 mg L^{-1}). Furthermore, metabolomics revealed that MPs exposure resulted in alterations of metabolic profiles and disturbed glycolysis, lipolysis and amino acid metabolism pathways in hepatopancreas of *L. vannamei*. This work confirms and expands the knowledge on the sublethal impacts and toxic modes of action of MPs in *L. vannamei*.

1. Introduction

In recent decades, large quantities of plastic debris have been continuously dumped into the ocean due to a lack of waste disposal awareness. In 2016, the global amount of plastic debris entering aquatic environments was estimated to be 19–23 million metric tons (mt), with a potential increase to 53 million mt by 2030 (Borrelle et al., 2020). Microplastics (MPs), which occur from the direct discharge of plastic microparticles and the environmental fragmentation of larger plastic debris, are anticipated to make up 13.5% of the marine plastic budget (Kane et al., 2020). This has led to increasing detection of high levels of MPs in surface seawater (around several thousand particles m^{-3}), particularly in coastal areas, harbors, estuaries, mangroves, etc. (Cai et al., 2018; Fu et al., 2020; Kang et al., 2015; Li et al., 2020a). The wide occurrence of MPs was also confirmed in marine sediments from coastal harbors, which would equate to MPs concentrations in pore water of 2.2–5.4 mg L^{-1} (Claessens et al., 2011). The enormous amounts of MPs in the ocean have raised global concern regarding their potential impacts on marine life and ecosystems.

Growing evidence has demonstrated the ingestion of MPs by aquatic animals such as fish (Lu et al., 2016), bivalves (Wang et al., 2021a), crustaceans (Saborowski et al., 2022), zooplankton (Jeong et al., 2016). The ingested MPs could accumulate in tissues over a long period of time due to their tiny size and poor biodegradability. The main ingestion pathways of MPs in aquatic animals include oral ingestion, respiration, and skin adherence (Kim et al., 2021; Kolandhasamy et al., 2018). The

* Correspondence to: Hainan Tropical Ocean University, No. 1 Yucai Road, Sanya 572000, China.
E-mail address: zengyx@hntou.edu.cn (Y. Zeng).

https://doi.org/10.1016/j.ecoenv.2023.114871
Received 5 January 2023; Received in revised form 30 March 2023; Accepted 3 April 2023
Available online 6 April 2023

primary uptake pathway of MPs in aquatic animals has been identified as gastrointestinal ingestion in bivalves and crustaceans (D'Costa, 2022; Valencia-Castañeda et al., 2022b; Wang et al., 2021a). The ingested MPs can rapidly accumulate in gastrointestinal tracts, cross the biological barriers, and translocate to other internal organs via the circulatory or lymphatic system (Kim et al., 2021). Gills are the respiratory organs that many aquatic organisms use to oxygenate their blood by extracting dissolved oxygen from water. Therefore, the large surface area of gill provides an uptake pathway for waterborne exposed MPs through respiration, microvilli activity and endocytosis (Von Moos et al., 2012). Notably, the morphological and physiological variations across aquatic species typically lead to discrepancies in the biodistribution and bioaccumulation features of MPs. Therefore, it is critical to investigate the characteristic MPs accumulation in specific aquatic species, identify organs with strong MP toxicity, and assess the relevant toxic modes of action.

Studies have shown that MPs accumulation in tissues could cause a number of adverse effects on the aquatic animals (D'Costa, 2022; Kögel et al., 2020). For instance, abundant accumulation of MPs in the digestive tract can result in physical blockages and mechanical injury in aquatic animals (Alimba and Faggio, 2019), which further causes reduced feeding, impaired behavior and inhibited growth and development (Wang et al., 2020). Long-term MP accumulation in fish gut can result in intestinal inflammation and oxidative stress, leading to the development of gut metabolic disorders due to intestinal microbiota dysbiosis (Kang et al., 2021; Qiao et al., 2019). Moreover, bioaccumulation of MPs in fish liver has been linked to hepatic inflammation, elevated oxidative stress (Feng et al., 2021; Lu et al., 2016), as well as disrupted hepatic glycolipid metabolism at various levels (Zhao et al., 2020). Accumulation of MPs in tissue also significantly impact other aquatic animals such as bivalves and crustaceans (D'Costa, 2022; Mkuye et al., 2022). Exposure studies have observed that ingestion of MPs can impair immune system functionality of bivalves by interfering with antioxidant systems, reducing phagocytosis, hemocyte count, and viability, as well as enhancing DNA damage (Mkuye et al., 2022). Additionally, MPs caused histological damage and alterations in the enzymatic biomarkers of lipid and energy metabolism in important organs, including the gill and digestive gland of bivalves, as well as disturbance of amino acid and glycerophospholipid metabolism pathways in the digestive gland (Teng et al., 2021).

Regarding marine crustaceans, recent research has begun to uncover potential effects of MPs accumulation on survival, growth, feeding, behavior, physiology, oxidative stress, microbial changes, etc. (Bergami et al., 2016; D'Costa, 2022; Wang et al., 2020, 2021b). For example, field studies have documented the ingestion of MPs in shrimp *Litopenaeus vannamei* and demonstrated the accumulation of MPs in gastrointestinal tract and gill, where the most abundant detected polymers were polyethylene, polyamide, and polystyrene (PS) (Valencia-Castañeda et al., 2022a, 2022b). Various toxicological studies have reported that accumulated MPs in tissues can lead to increased mortality, reduced feeding rate and altered swimming behavior of crustaceans as reviewed by D'Costa (2022). Moreover, the retention of MPs in tissues can exert an influence on the antioxidant system, leading to oxidative damages and histopathology injuries in *L. vannamei* (Hsieh et al., 2021), as well as activation of the expression of antioxidant genes and regulation of the MAPK signaling pathway in crab *Eriocheir sinensis* (Yu et al., 2018). Recent studies also found that MPs exposure can induce immune defense response and dysbiosis of microflora in *L. vannamei* (Wang et al., 2021b), and alter protein and metabolic profiles in hemolymph of *L. vannamei* (Duan et al., 2021). However, there are a few systematic studies focusing on the toxic modes of action underpinning MPs-induced toxicological consequences on marine crustaceans, especially from the aspects of cellular and molecular levels.

Litopenaeus vannamei (whiteleg shrimp), a penaeid shrimp genus, widely distributed along Pacific coast, is now the top cultivated and globally traded crustacean species with substantial economic value. In 2020, the annual global production of *L. vannamei* reached 5.8 million tons with an estimated value of USD 24.7 billion, making up 51.7% of the total farmed crustacean species (FAO, 2022). The plastic wastes generating from aquaculture and fisheries activities along with other terrestrial anthropogenic sources, are increasingly entering the aquaculture ecosystems, posing a great threat to the well-being and sustainability of *L. vannamei*. Therefore, *L. vannamei* was selected as the test organism in the current study. Polystyrene (PS) microspheres were selected as MPs for the exposure experiments, since PS is one of the most manufactured plastics and most prevailing polymer types of MPs detected in marine crustaceans (Alimba and Faggio, 2019; Hara et al., 2020; Valencia-Castañeda et al., 2022b). This study hypothesized that *L. vannamei* can ingest and accumulate PS MPs in specific organs, leading to a variety of toxic effects at the behavioral, histological and biochemical levels. Herein, *L. vannamei* were exposed to waterborne MPs at environmentally relevant concentrations. The accumulation and distribution of MPs in the organs were determined by fluorescence tracing. Behavior monitoring, enzymatic biomarker assay, histopathological analysis and metabolomic profiling were jointly conducted to unravel the interlinked toxicological consequences and relevant mechanisms of MPs on *L. vannamei*.

2. Experimental

2.1. Animals and MPs

Healthy whiteleg shrimp postlarvae (*L. vannamei*, 1–2 cm body length, 25-day-postlarvae (PL25)) were obtained from Hainan Zhongzheng Aquatic Products Technology Co., Ltd (Hainan, China) and were subsequently cultured in artificial seawater (ASW, composition of ASW shown in Table S1) with a salinity of 20 ± 1‰ by using aquatic sea salt (Blue treasure, China) and de-ionized water. The individuals were fed with a commercial diet formulated for whiteleg shrimp (5% of body weight, Guangdong Yuehai diet Co., Ltd, Guangdong, China) daily. During the acclimation period, the organisms were maintained in aquariums for three weeks under laboratory conditions (light/dark cycle (12 h/12 h), temperature: 28 ± 1 °C; pH: 7.6 ± 0.1; dissolved oxygen: 7.4 ± 0.3 mg L^{-1}).

Polystyrene (PS) microspheres with uniform diameter of 2 μm were purchased from BaseLine ChromTech Research Centre (Tianjin, China). Although field study showed that most abundant MPs spheres detected in shrimps ranged from 10 to 20 μm in diameter (Curren et al., 2020), many environmental MPs occur as small secondary MPs derived from plastics degradation, which are hardly detected in field study due to technique limitations (Barbosa et al., 2020). Therefore, small PS size (2-μm diameter) was selected in this study considering environmental plastics degradation, which normally exhibit higher bioavailability to organisms than larger MPs, but their toxicological effects remain largely unexplored (Dawson et al., 2018; Lee et al., 2013). The fluorescent-labeled PS microspheres (2-μm diameter) were used to track the bioaccumulation and biodistribution of PS in the organism (excitation wavelength: 488 nm; emission wavelength: 518 nm). The virgin PS microspheres (2-μm diameter) without fluorescence were employed for the chronic toxicity test. The polymer composition of the MPs was examined by micro-Raman spectroscopy (DXR™, Thermo-Fisher Scientific) (Fig. S1). The size and morphology of the PS microspheres were characterized by transmission electron microscopy (Tecnai G2 F20, FEI, Netherlands) (Fig. S1). The MPs stock solution of 1.0 mg mL^{-1} was prepared using ASW. The prepared stock solution was treated in an ultrasonic bath prior to use.

2.2. MPs accumulation and distribution

To assess the accumulation, distribution and elimination of MPs, healthy acclimated *L. vannamei* juveniles (4.4 ± 0.4 cm in body length, 0.49 ± 0.06 g in body weight) were randomly cultured in 3 glass tanks in

triplicate (one control and two treatments). The control consisted of a total of 24 individuals distributed in 3 tanks (8 ×3) containing 2.5 L of pure ASW each without MPs and without a depuration cycle after 48 h exposure. The two treatments consisted of 48 individuals equally distributed in 6 tanks (8 ×6) containing 2.5 L of ASW each and spiked with fluorescent MPs at a concentration of 1.0 mg L^{-1}. This concentration is the same as the highest MPs concentration (1.0 mg L^{-1}) used in the subsequent chronic toxicity test, which reflects the environmental MPs concentrations in surface seawater from coastal areas, harbors, estuaries, mangroves (e.g., 3.7 mg L^{-1}) (Cai et al., 2018; Fu et al., 2020; Kang et al., 2015; Li et al., 2020a) and in pore water of marine sediments from coastal harbors (2.2–5.4 mg L^{-1}) (Claessens et al., 2011). The experiments for the first treatment (8 ×3) were terminated after 48 h MPs exposure. In contrast, the experiments for the second treatment (8 ×3) were submitted to a 48-h depuration cycle after the initial 48 h MPs exposure. During the experiment, all shrimps were fasted and the solution in each tank was changed daily. All other conditions remained the same as the acclimation period. After the experiment, shrimps were euthanized on ice, and different organs (gill, gut, stomach and hepatopancreas) were collected for subsequent analyses.

In order to ascertain the MPs ingestion by *L. vannamei* and to observe the biodistribution of MPs in various organs (gill, gut, stomach, hepatopancreas), the collected organs were fixed in 4% paraformaldehyde, embedded in paraffin wax and sectioned at 4 μm thickness for microscopic observation. The analyses were performed with a laser scanning confocal microscope (Nikon, Eclipse Ti, Japan) using a 480 nm laser source. The obtained images were processed by Image J software (http://imagej.net/, version 1.53k) to calculate the particle size.

For quantitative analyses of MPs, the tissues of shrimps were stored at − 20 °C. The tissues of two individuals were pooled as one sample and three replicates were performed for the analyses. Each sample was weighed and digested in 8 mL of 10% KOH solution at 60 °C for 48 h. The digestion protocol was slightly modified based on a previous study (Dehaut et al., 2016), which offered an efficient digestion of seafood tissues without evident degradation on MPs polymers. The resulting digestion solution was diluted with deionized water to 8 mL and its fluorescent intensities were determined in triplicate using a fluorescence spectrophotometer (Agilent Cary Eclipse G9800A) with excitation wavelength at 488 nm. The contents of MPs accumulated in various tissues were quantified based on the standard curve built by a series of fluorescent MPs solution (Fig. S2). The final results were presented as mass concentration μg (particle)/mg (wet weight) (precision (CV%), 4.1%–12.4%).

2.3. Toxicity experiment

For the toxicity test, healthy acclimated *L. vannamei* juveniles (4.4 ± 0.4 cm in body length, 0.49 ± 0.06 g in body weight) were randomly assigned into one control group and three MPs exposure groups with five replicate glass tanks for each group (8 individuals in one tank). The shrimps were exposed in 3 L glass tanks with 2.5 L of test solution for 8 days. This exposure duration was selected considering the molting interval of *L. vannamei* (around 4–6 days at juvenile stage) which is crucial physiological process in their life cycle, so as to span at least one cycle of molting during the exposure period (Betancourt-Lozano et al., 2006; Corteel et al., 2012). Individuals in the control group were exposed in ASW prepared as described above, while individuals in the MPs exposure groups were exposed to PS MPs in ASW at concentrations of 0.02 mg L^{-1} (PS-L), 0.2 mg L^{-1} (PS-M) and 1.0 mg L^{-1} (PS-H), respectively. These exposure concentrations represent MP concentrations found in surface seawaters from coastal areas, harbors, estuaries, mangroves as well as the lower range of MP concentrations commonly employed in exposure experiments (Cai et al., 2018; Fu et al., 2020; Lenz et al., 2016; Li et al., 2020a; Phuong et al., 2016). All the other conditions remained the same as the acclimation period. The individuals were fed with a commercial formulated diet (5% of body weight) once a day as described above. After 8 days of exposure, the shrimps were used for subsequent analyses including swimming behavior test (alive shrimps), histopathological analysis (samples were fixed in 4% paraformaldehyde), biochemical and metabolomic analyses (samples were frozen in liquid nitrogen and transferred to −80 °C), respectively.

2.4. Swimming behavior test

After the toxic exposure period, shrimps were randomly taken out from each group for the assessment of swimming behavior (12 individuals used for each group, 4 individuals per tank for each replicate). They were subsequently transferred into 30 × 18 × 20 cm (L× W × H) glass tanks containing 2 L of test solution. To record their swimming behavior, a video camera (Sony, FDR-AX60, Japan) was fixed by the camera frame installed on the top of glass tank to ensure the capture of the whole rectangular tank bottom at the same position. The behavior test was run in triplicate. For each test, the swimming behavior of four shrimps from each group was recorded simultaneously for 4 min after 5 min of acclimation (Wang et al., 2020). The recorded videos were processed by an automated image-based tracking software ToxTrac (Umeå university, Umeå, Sweden), which can track multiple organisms simultaneously with the preservation of their identity in the laboratory environment and yield basic behavioral parameters in a robust and time-efficient manner (Rodriguez et al., 2018). The average speed, total distance traveled and exploration rate of each individual in each tank were measured and exported in Excel format. Average speed was defined as average of instantaneous speed in mm s^{-1}. Total distance traveled represented the total swimming distance in mm. Exploration rate was presented as the percentage of number of explored areas divided by number of total areas. These parameters were further visualized by bar graphs and heat maps. The heat maps are color coded according to the normalized representation of the frequency of use in the linear scale and shown superimposed to the arena picture (i.e., rectangular tank bottom) in real scale (Rodriguez et al., 2018).

2.5. Biochemical analysis

The antioxidant defense system of *L. vannamei* were investigated by measuring the responses of oxidative stress relevant biomarkers including superoxide dismutase (SOD), catalase (CAT), glutathione peroxidase (GPx) activity and malondialdehyde (MDA) to MPs exposure (n = 3–6). In addition, indicator of neurotoxic response, i.e., acetylcholinesterase (AChE) was measured. These biomarkers and the total protein content were analysed with commercial detection kits, of which enhanced bicinchoninic acid assay (BCA) protein assay kit, total SOD assay kit with WST-8, CAT assay kit, cellular GPx assay kit with NADPH and lipid peroxidation MDA assay kit were from Beyotime biotechnology (Shanghai, China) and AChE assay kit was from Jiancheng Bioengineering Institute (Nanjing, China) (details of these kits shown in supplementary material). Three shrimps were pooled as one sample and each sample was homogenized in sufficient ice-cold homogenization buffer by a tissue homogenizer (Tissuelyser, Shanghai, China). The homogenates were centrifuged at 10,000 g for 15 min at 4 °C. The supernatants were subsequently collected for the determination of biomarkers. The experimental operations were performed based on the manufactures' protocols and the measurements were conducted by a spectrophotometer equipped with a microplate reader (Thermo Scientific™ Varioskan™ Flash).

2.6. Histopathological analysis

The hepatopancreas of *L. vannamei* from various groups (n = 3 for each group, 3 tissue slices for each sample) were dissected and fixed in 4% paraformaldehyde immediately. The fixed tissues were embedded in paraffin wax, sectioned at 4 μm thickness, and stained with hematoxylin and eosin (H&E). The tissue slices were observed under microscopy to

assess hepatopancreas damage by histopathological analysis, which were evaluated semi-quantitatively by ranking the severity of lesions as described previously (Lin et al., 2022).

2.7. Metabolomics analysis

The hepatopancreas of three *L. vannamei* were pooled as one sample and six replicates were conducted for each group. The metabolites extraction protocol was adapted from a previous study (Fu et al., 2018). Briefly, the hepatopancreas tissues (40 ± 1 mg) were homogenized with 400 μL ice-cold Milli-Q water and spiked with 800 μL methanol/acetonitrile (1:1, v/v), followed by ultrasound-treatment for metabolites extraction. The prepared metabolite extracts were subjected to the liquid chromatography-tandem mass spectrometry (LC-MS/MS) analysis using ultra-high performance liquid chromatography (UPLC) system coupled with an Orbitrap Q Exactive Focus mass spectrometer (Thermo Fisher Scientific, USA). The chromatographic separation was performed on a Hypersil Gold C_{18} column using a binary mobile phase system (A: water, B: acetonitrile). The mass spectrometry data were acquired using electrospray ionization in the negative and positive ionization modes. The LC-MS/MS raw data were processed by Compound Discover 3.1 (Thermo Fisher Scientific, USA) for assignment, extraction, alignment, identification and area integration of the peaks. Detailed sample preparation and instrumental parameters were provided in supplementary material.

2.8. Statistical analysis

The univariate statistical analyses were conducted by SPSS 21.0 software. The normality of data and the homogeneity of the variances were assessed by one-sample Kolmogorov-Smirnov test and Levene's test. Afterwards, one-way ANOVA followed by Tukey's post-hoc test was performed to assess the statistical differences of various parameters among various treatments. The multivariate statistical analyses of metabolomic data were conducted by SIMCA 14.1.0 (Umetrics, Sweden). The metabolomic data were first examined by principal component analysis (PCA) to detect groupings and outliers. Next, partial least squares - discriminant analysis (PLS-DA) model was constructed for four groups to elucidate the trends of metabolic alterations induced by the different treatments. The obtained PLS-DA model was validated based on CV-ANOVA PLS scores to test for significance. Metabolites with variable importance in the projection (VIP) > 1 and univariate $p < 0.05$ were considered as significantly altered metabolites in the MPs exposure groups compared to control group. A heat map was generated by MetaboAnalyst 5.0 (www.metaboanalyst.ca/) to present the pattern of metabolic changes of significantly differed metabolites between the control and treatment groups.

3. Results

3.1. Distribution and accumulation of MPs

Fluorescence tracer technique was used to track the distribution and accumulation in various organs of *L. vannamei*. The results obtained from histological sections of exposed shrimps by laser scanning confocal microscopy showed that MPs particles were clearly observed in gill, stomach, gut and hepatopancreas and their distribution characteristics in various organs were captured (Fig. 1, Table S2). In gill small MPs with average size of 1.98 ± 0.31 μm were scattered in the gill filament (Fig. 1A), whereas several large fluorescent MPs spots (size 14.7–25.5 μm) along with many tiny MPs spots were clearly visualized in stomach (Fig. 1B). Concerning the gut, the observed MPs spots (1.26 ± 0.38 μm in size) were basically smaller than the exposed MPs (2 μm in size), with the exception of the two largest MPs spots (3.5 μm and 2.2 μm in size), which were slightly larger than the exposed MPs (Fig. 1C). In hepatopancreas, many tiny MPs with size similar to the exposed MPs were detected inside the hepatopancreas tubules (Fig. 1D); moreover, two large fluorescent spots (size 21.0 μm and 19.6 μm) were aggregated

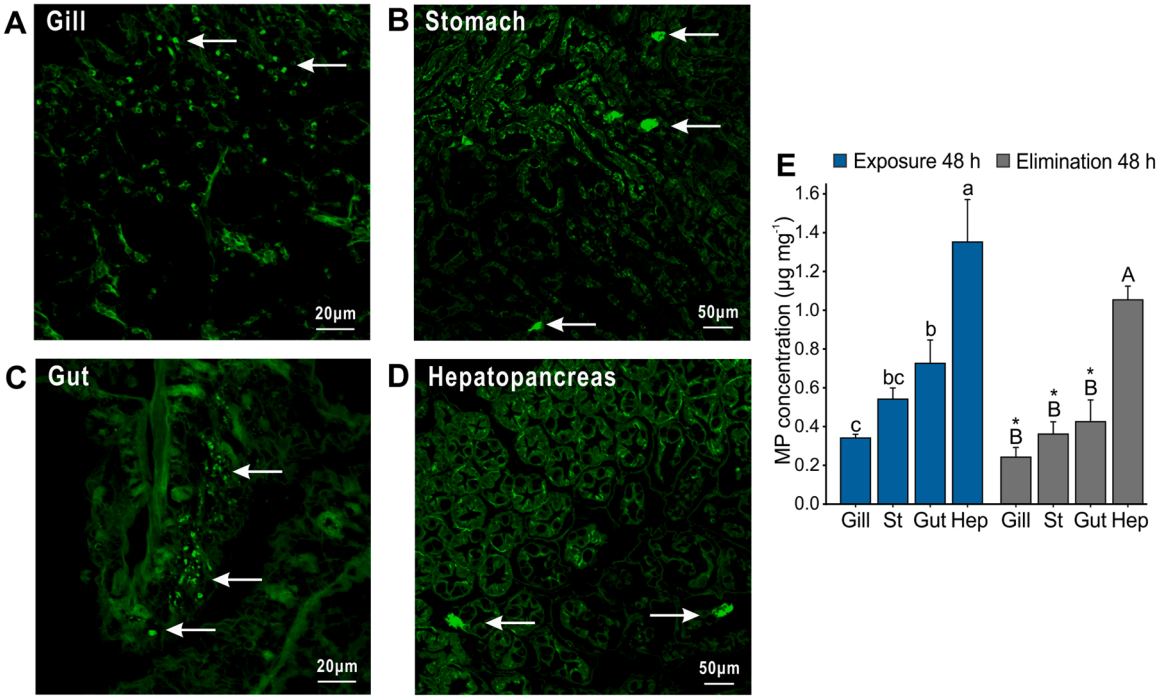

Fig. 1. Distribution and accumulation of fluorescent MPs in various organs of *L. vannamei* exposed to 1.0 mg L^{-1} MPs. Green fluorescent MPs were observed in gill (A), stomach (B), gut (C) and hepatopancreas (D) of *L. vannamei* by laser scanning confocal microscopy. The white arrows indicate typical MP spots in the organs. (E) Concentrations of MPs in various organs of *L. vannamei* after periods of exposure and elimination of 48 h (St: stomach; Hep: hepatopancreas). Values are means ± SD (n = 3). Different letters represent significant differences among concentrations of MPs in different organs, and asterisks indicate significant differences of the concentration of MPs in specific organ between two time points ($p < 0.05$, ANOVA followed by Tukey's post-hoc test).

adjacent to hepatopancreas tubules.

The contents of MPs in different organs were quantified by fluorescence spectrophotometer (Fig. 1E). It can be observed that the accumulation of MPs in hepatopancreas was more abundant than that in gill, stomach and gut during both the exposure and elimination periods ($p < 0.05$) (Fig. 1E). The content of MPs accumulated in gut was significantly higher than that in gill ($p < 0.05$). After elimination period, the contents of MPs in gill, stomach and gut significantly decreased ($p < 0.05$), while the MPs accumulation in hepatopancreas was not significantly lowered after elimination (Fig. 1E). Notably, the distribution tendency of MPs in various organs remained similar before and after the depuration period although the ingested MPs were depurated to some extent.

3.2. Survival, growth and swimming behavior

For toxicity test, no significant difference was found for survival rate among various groups (Fig. S3). However, compared with controls, the growth of *L. vannamei* was inhibited by 52.1% when exposed to the highest MPs concentration (PS-H, 1.0 mg L^{-1}) (Fig. S3). The effects of MPs on the swimming behavior of *L. vannamei* were shown in Fig. 2. Compared with controls, MPs exposure at three concentrations significantly decreased the average swimming speed of *L. vannamei* by 43.7% (PS-L), 57.9% (PS-M) and 80.2% (PS-H), respectively (Fig. 2A). Similarly, a distinct concentration-dependent effect was detected for the total swimming distance, where MPs exposure significantly reduced the total swimming distance by 39.6% (PS-L), 55.3% (PS-M) and 79.9% (PS-H), respectively, relative to that of control group (Fig. 2B). As for the exploration rate, only MPs exposure at the highest concentration significantly decreased the exploration rate of shrimps comparable to that of control group (Fig. 2C). The swimming range and frequency of *L. vannamei* in various groups were also monitored using animal behavioral tracking software ToxTrac and subsequently visualized by heatmaps (Fig. 2D-G). The shrimps in the control group generally displayed a wider swimming range and a higher swimming frequency compared to those MPs exposure groups. In particular, the shrimps in the PS-H group explored the least space among all the groups (Fig. 2G). Additionally, the shrimps in the MPs exposure groups showed a tendency of swimming in a wall-sticking manner.

3.3. Biomarker responses

The levels of a series of biomarkers in *L. vannamei* were examined to study the oxidative stress, lipid peroxidation, and neurotoxicity induced by various concentrations of MPs (Fig. 3). Compared with controls, SOD activity displayed a rising trend after MPs exposure, and it was significantly elevated in the PS-H group ($p < 0.05$) (Fig. 3A). In contrast, CAT activity exhibited a concentration-dependent downward trend after MPs

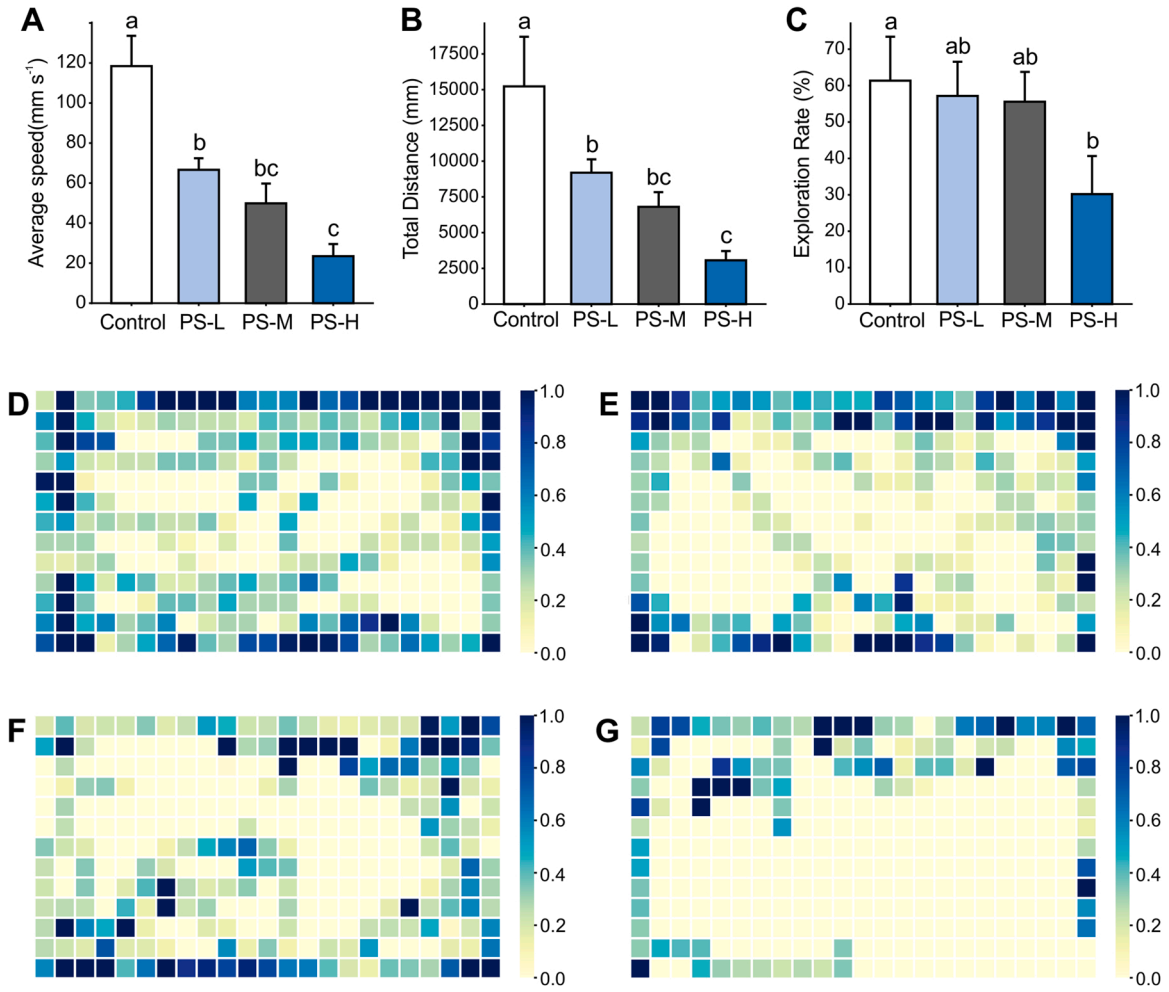

Fig. 2. Swimming behavior and performance of *L. vannamei* after MPs exposure. Average speed (A), total distance (B) and exploration rate (C) of *L. vannamei* after exposed for 8 days to 0 (control), 0.02 mg L^{-1} (PS-L), 0.2 mg L^{-1} (PS-M) and 1.0 mg L^{-1} (PS-H) MPs. Values are means ± SD (n = 3). Different letters indicate significant differences among concentrations of MPs different organs ($p < 0.05$, ANOVA followed by Tukey's post-hoc test). The heat maps represent the swimming range and frequency of *L. vannamei* in control (D), PS-L (E), PS-M (F) and PS-H (G) groups measured during 4 min in aquarium. The x- and y-axes are shown superimposed to the arena picture (i.e., rectangular aquarium bottom) in real scale. Color intensity bar indicates the swimming frequency of *L. vannamei*.

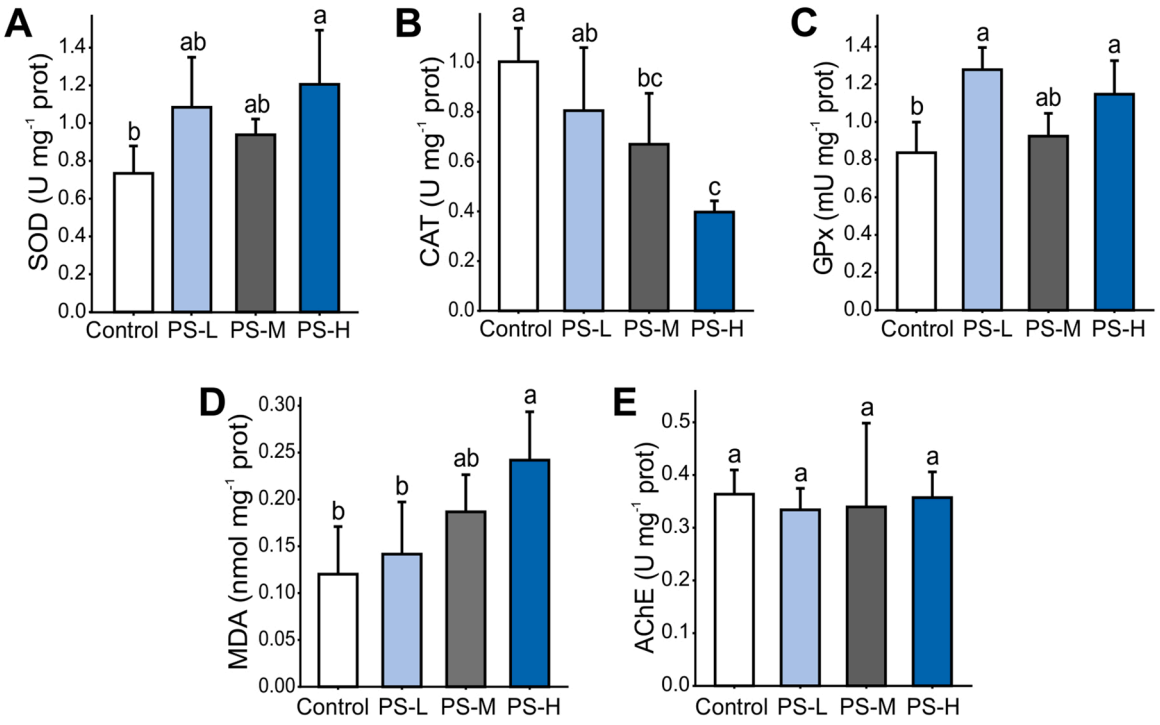

Fig. 3. Effects of MPs exposure on biomarkers of oxidative stress and neurotoxicity in *L. vannamei*. (A) SOD activity; (B) CAT activity; (C) GPx activity; (D) MDA levels; (E) AChE activity. Values are means ± SD (n = 3–6). Different letters indicate significant differences among treatments ($p < 0.05$, ANOVA followed by Tukey's post-hoc test).

exposure ($p < 0.05$) (Fig. 3B). Notably, strong positive correlations were observed between CAT activity and swimming performance parameters including average swimming speed ($r = 0.804$, $p < 0.01$) and total swimming distance ($r = 0.727$, $p < 0.01$) (Table S3). The exposure at low and high concentrations of MPs induced significant increases in GPx activities compared to control group ($p < 0.05$) (Fig. 3C). In addition, MDA levels developed concentration-dependent increasing responses following MPs exposure, where the exposure at highest concentration of MPs induced significant increases in MDA levels compared to controls ($p < 0.05$) (Fig. 3D). Moreover, MDA level was highly correlated to average swimming speed ($r = -0.748$, $p < 0.01$) and total swimming distance ($r = -0.762$, $p < 0.01$) (Table S3). As for the AChE levels, no significant difference between various groups was observed (Fig. 3E).

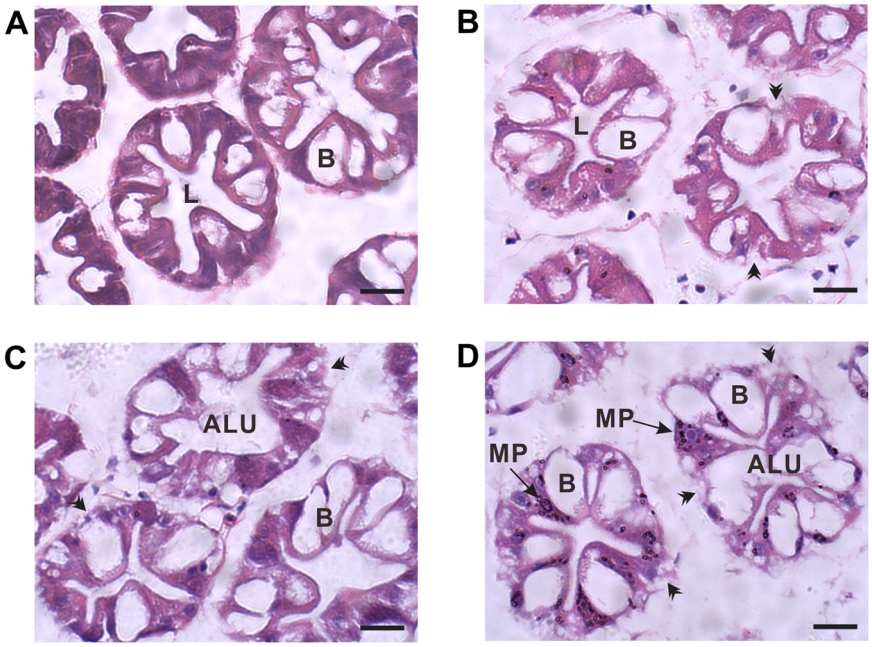

Fig. 4. Histological observations in hepatopancreas of *L. vannamei* after MPs exposure. Bar scale (20 μm). (A) control; (B) PS-L, 0.02 mg L^{-1}; (C) PS-M, 0.2 mg L^{-1}; (D) PS-H, 1.0 mg L^{-1}. Abbreviations: B (B-cells, secretory cells), L (star-shaped lumen), ALU (abnormal lumen), MP (microplastics), black arrow head (cytolysis).

3.4. Histological observations

The microscopic examination revealed that the hepatopancreas of *L. vannamei* from the controls displayed well-defined structure of tubules, lumen and cells (Fig. 4A). After exposure to low concentration of MPs, the general morphological structure of hepatopancreas was close to the control group and the star-shaped tubular lumen were still preserved in the hepatopancreas of PS-L group; however, the tubules showed a loose arrangement, some of the epithelial cells became ruptured (Fig. 4B). When exposed to the medium concentration of MPs, distorted and deformed lumen, increased size of B-cells and epithelial cell cytolysis were clearly observed in the hepatopancreas of PS-M group (Fig. 4C). Particularly, the exposure to high concentration of MPs caused evident accumulation of MPs in the tubular epithelial cells, which eventually resulted in severe histopathological changes in the hepatopancreas of PS-H group including tubular atrophy, loose arrangement of tubules, loss of the star-shaped lumen structure, epithelial cell cytolysis, and deterioration in the integrity of the tubular structure (Fig. 4D). The semi-quantitative degree of histological changes in the hepatopancreas of *L. vannamei* was summarized in Table 1.

3.5. Metabolic changes

The LC-MS/MS metabolomics approach characterized 119 metabolites in the hepatopancreas of *L. vannamei*, which included amino acids, fatty acyls, lipids, peptides, acylcarnitines, nucleic acids, organic acids. The initial exploratory inspection by PCA presented a good overview of the structure in the data, which showed a proper class grouping of four groups on scores plot after excluding two outliers (Fig. S4). The PLS-DA model was constructed for all groups to elucidate the metabolic alterations induced by the different exposure conditions (CV-ANOVA, $p = 0.01$). The scores plot showed that the metabolic profiles between control and MPs exposure groups were well separated (Fig. 5A). This indicated that MPs exposure caused evident metabolic alterations in the hepatopancreas of *L. vannamei* which varied with the concentrations of MPs. The loadings plot revealed the main metabolites responsible for the discrimination of metabolic profiles of various groups from the aspects of the two loadings (Fig. S5). The differential metabolites among four groups were identified by both univariate and multivariate approaches and their alteration patterns within various groups were visualized by heatmaps (Fig. 5B). For example, glyceraldehyde was significantly downregulated in the hepatopancreas of MPs exposure groups compared with controls. Fatty acids, including 3-methyladipic acid, azelaic acid, suberic acid, adipic acid, sebacic acid, leucinic acid, 2-hydroxymyristic acid, were significantly downregulated due to exposure to low concentration of MPs. Meanwhile, MPs exposure caused pronounced changes in the levels of several acylcarnitines. Furthermore, the levels of amino acids and dipeptides, such as taurine, L-aspartic acid, N-acetyl-L-alanine, were significantly upregulated after MPs exposure at all concentrations. The main metabolic pathways disturbed by MPs exposure were summarized in Fig. 6. Metabolic pathway analysis further demonstrated that MPs exposure could influence glycolysis, lipolysis and amino acid metabolism pathways.

Table 1
Semi-quantitative evaluation of histological changes in hepatopancreas of *L. vannamei* exposed to 0 (control), 0.02 mg L^{-1} (PS-L), 0.2 mg L^{-1} (PS-M) and 1.0 mg L^{-1} (PS-H) MPs.

Histological observation	Control	PS-L	PS-M	PS-H
Loose arrangement of tubules	+	++	+	+++
Degenerated tubular structure	–	+	+	+++
Hepatic epithelial cell cytolysis	–	+	++	+++
Increased size of B-cells	+	++	+++	+++
Loss of the star-shaped lumen structure	–	–	++	+++

Note: (–) absent; (+) weak; (++) moderate; (+++) strong.

4. Discussion

4.1. Distribution and accumulation of MPs in L. vannamei

To identify organs with significant MP toxicity and explore the underlying mechanisms, it is crucial to investigate the distribution and accumulation features of MPs in organisms. Our results demonstrated the uptake and accumulation of MPs in gill, stomach, gut and hepatopancreas of *L. vannamei*, but with different distribution characteristics of MPs among various organs. In gill, the observed MPs size is similar to the exposed MPs size (2 μm), suggesting that *L. vannamei* could ingest MPs predominantly in their pristine forms. This is consistent with previous findings of MPs accumulation in the gills of fish (Lu et al., 2016), bivalves (Li et al., 2020b; Wang et al., 2021a) and crustaceans (D'Costa, 2022). In stomach and hepatopancreas, the most evident phenomenon was the significantly greater size of several fluorescent MPs spots than the pristine MPs. Similar phenomena were observed in other studies employing bivalves as MPs exposure animal models (Li et al., 2020b; Wegner et al., 2012), which could be attributed to the homo-aggregation of MPs in organisms and hetero-aggregation of MPs interacted with biomacromolecules in *L. vannamei* (Alimi et al., 2018; Li et al., 2020b; Saborowski et al., 2022). Moreover, many tiny MPs (<1 μm) occurred in the digestive system of *L. vannamei*, which could be explained by mechanical disruption of MPs by gastric mills as well as the aid of digestive enzymes (Dawson et al., 2018). For example, Antarctic krill can fragment most of the ingested MPs (31.5 μm) into smaller pieces (<1 μm) that are directed to gut for excretion (Dawson et al., 2018). This degradation process could facilitate the internalization of small MPs by endocytosis in epithelial cells and enhance the capacity of small MPs for crossing biological barriers, thus affecting the bioavailability and toxicity of MPs (Zitouni et al., 2021).

Our quantitative results further revealed the accumulation characteristics of MPs in *L. vannamei*, i.e., the 2 μm MPs tended to be accumulated mostly in hepatopancreas, followed by gut, stomach and gill. The digestive tract of shrimp consists of esophagus, stomach, hepatopancreas and gut (Sousa and Petriella, 2006). Thus, the observed accumulation tendency suggested that the internal digestive system rather than gill is the main target organ of MPs accumulation, which corresponds well with laboratory studies of MPs accumulation on bivalves and fish through quantification by fluorescence spectroscopy (Kolandhasamy et al., 2018; Lu et al., 2016; Wang et al., 2021a). Moreover, recent field studies have found that both wild and farmed shrimp *L. vannamei* show a similar pattern of accumulation of MPs greater in the digestive tract than in other tissues (Valencia-Castañeda et al., 2022a, 2022b), where the estimated MPs concentrations in the hepatopancreas and gill were highly comparable to our study. This tendency has also been observed in some studies on the ingestion and translocation process of MPs in other shrimp species by fluorescence microscope. For instance, administration of differently sized fluorescent MPs showed that Atlantic ditch shrimp (*Palaemon varians*) could accumulate 9.9 μm MPs in the stomach and gut, while smaller MPs (2.1 and 0.1 μm) could travel through the pyloric filter and be further transported into the internal tissues, such as hepatopancreas (Saborowski et al., 2022). Similar results were obtained in the present study, where small exposed MPs (2 μm) can be easily ingested and accumulated in the stomach, then egested through the gut after elimination process. In the digestive tract, MPs undergo biological degradation and mechanical disruption, which fragment them into smaller MPs and even nanoplastics (Dawson et al., 2018). This process facilitates the translocation of MPs into the hepatopancreas, making the hepatopancreas the most abundant organ for MPs accumulation. Moreover, the accumulated MPs tend to be retained in the hepatopancreas even after the elimination process. Since the hepatopancreas functions as the main organ for nutrient resorption and digestive enzyme synthesis, the accumulated MPs in hepatopancreas tubules could induce severe cytotoxic responses (Saborowski et al., 2022). Accordingly, our data showed that the

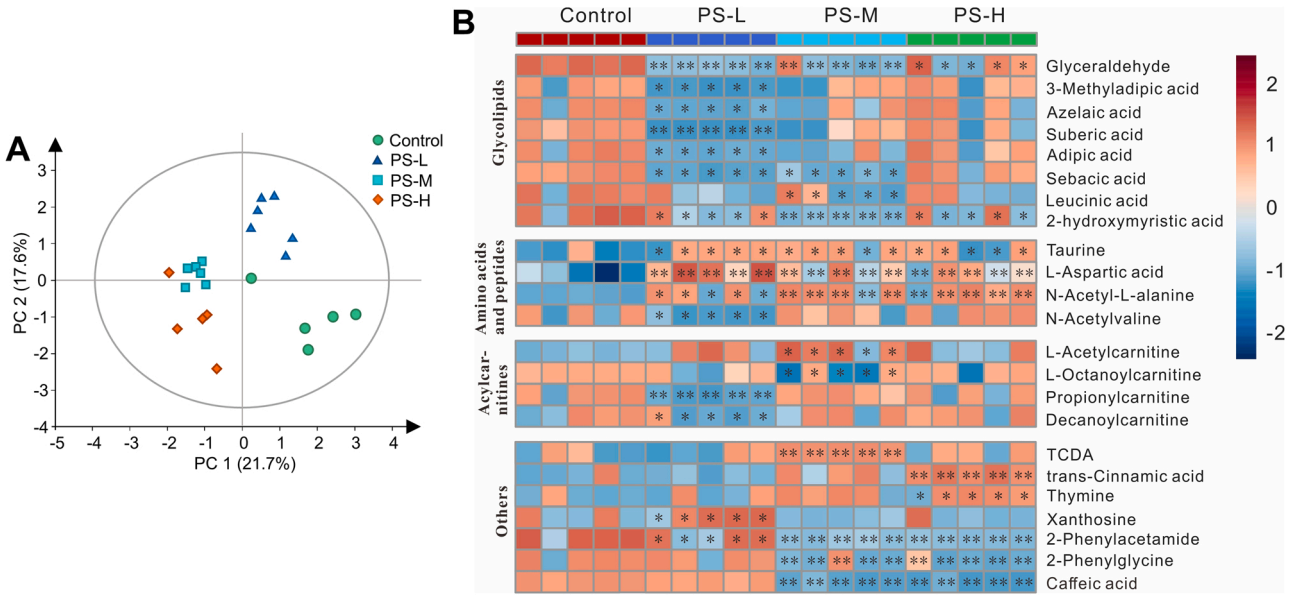

Fig. 5. Metabolic alterations induced by different concentrations of MPs in hepatopancreas of *L. vannamei*. (A) The PLS-DA scores plot for metabolic profiles of hepatopancreas of *L. vannamei* exposed to 0 (control), 0.02 mg L^{-1} (PS-L), 0.2 mg L^{-1} (PS-M) and 1.0 mg L^{-1} (PS-H) MPs. (B) Heat map for differential metabolites in the hepatopancreas of *L. vannamei* identified between the control and treatment groups. The color bar represents the relative content of metabolites based on z-scores. Asterisks indicate significant differences in the levels of metabolites between the control and treatment groups (* $p < 0.05$ and VIP ≥ 1; ** $p < 0.01$ and VIP ≥ 1). Abbreviations: TCDA, taurochenodesoxycholic acid.

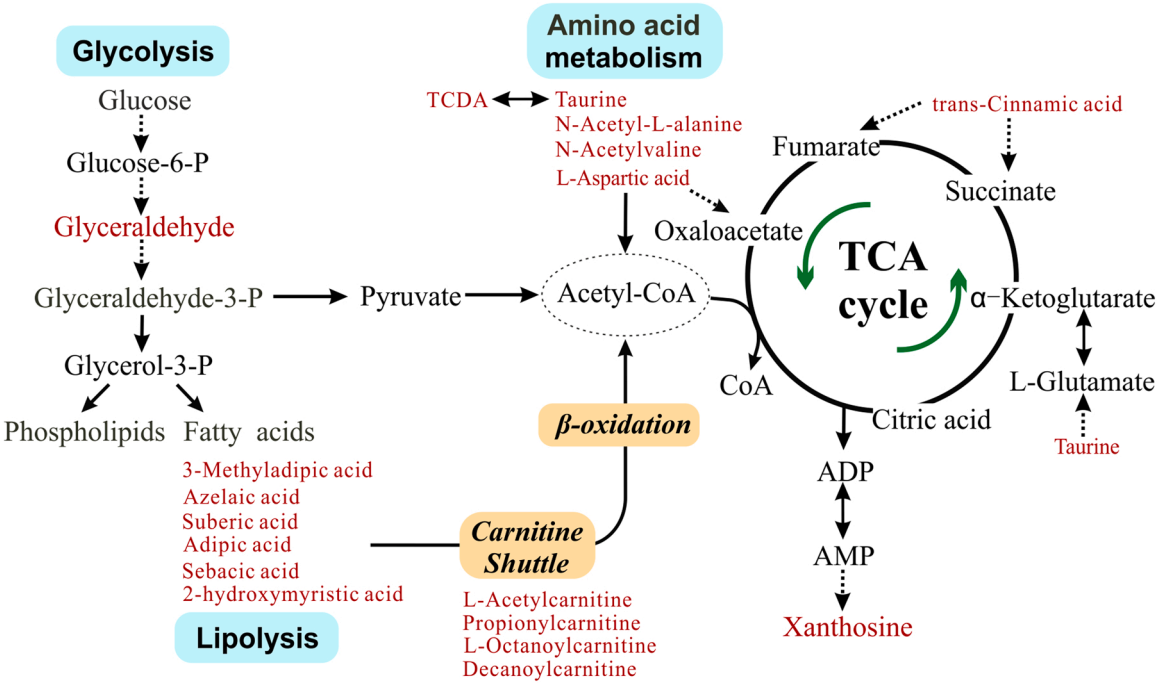

Fig. 6. Pathway analysis of common differential metabolites in the hepatopancreas of *L. vannamei* induced by MPs exposure. The compounds colored in red indicate the significantly altered metabolites detected in current study. The processes highlighted in light blue represent the main metabolism pathways linked to these altered metabolites. Abbreviations: TCA, tricarboxylic acid; TCDA, taurochenodesoxycholic acid.

aggregation of MPs in the hepatopancreas led to the disintegration of adjacent hepatopancreas tubules, causing cell damage and further induced tubules necrosis in the hepatopancreas.

4.2. Effects of MPs on the survival and growth of *L. vannamei*

In this study, MPs accumulation did not significantly affect the survival of *L. vannamei* at three concentrations (from 0.02 to 1.0 mg L^{-1}) after 8 d exposure, in agreement with previous researches on brine shrimps exposed to a series of 0.1 μm PS MP (from 0.001 to 10 mg L^{-1}) for 48 h (Gambardella et al., 2017) and 40 nm carboxylated PS (PS-COOH) MPs up to 10 mg L^{-1} for 14 d (Bergami et al., 2017). Previous study showed that the survival rate of *L. vannamei* was not affected by exposure to lower concentrations of polyethylene MPs (0.05 and 0.5 mg L^{-1}) for 48 h, but was significantly reduced when exposed to high concentration of polyethylene MPs (5.0 mg L^{-1}) (Wang et al., 2021b).

These findings indicate that MPs exposure conditions (time and concentration), particle properties (size, polymer type and shape) and species differences are important factors that contribute to the inconsistent toxic responses of organisms (Kögel et al., 2020).

Notably, MPs accumulation caused sub-lethal effects such as physiological, pathological and biochemical effects which may affect the survival of *L. vannamei* after prolonged period. The results showed that growth inhibition of *L. vannamei* was only observed following high concentration of MPs exposure (1.0 mg L^{-1}), which may occur in some heavily polluted coastal areas, harbors and estuaries with MPs concentrations in surface seawater up to 3.7 mg L^{-1} (Cai et al., 2018; Fu et al., 2020; Kang et al., 2015). After MPs exposure, the abundant MPs accumulation in the digestive system of *L. vannamei* may cause gastrointestinal tract blockage, mechanical and functional injury thus reducing feeding and nutrient absorption, which ultimately lead to growth inhibition of *L. vannamei* (Cole et al., 2015; Watts et al., 2015). Similarly, the ingestion of both PS and PS-COOH MPs caused growth inhibition of mysid shrimp larvae in a concentration-dependent mode, which could be attributed to reduced food intake and energy deficiency in response to accumulated MPs in the stomach (Wang et al., 2020). Weathered polyethylene MPs exposure also inhibited the growth of whiteleg shrimp, and this impact was intensified with increasing concentration and duration (Hariharan et al., 2022).

4.3. Effects of MPs on the swimming behavior of L. vannamei

Swimming behavioral responses to toxic exposure conditions were demonstrated to be a sensitive indicator in various invertebrates including crustaceans (Gambardella et al., 2017). Our results showed that 8 days of MPs exposure at all concentrations exert a significant impact on the whole swimming performance of *L. vannamei* (e.g., reduced average swimming speed and total swimming distance). The organisms displayed abnormal behavior changes characterized by wall-sticking swimming manner and decreased explorative activity particularly following high concentration of MPs exposure (1.0 mg L^{-1}), probably indicating avoidance behavior against the hostile environment. Several reasons might account for the above phenomena. First, MPs adherence on the surface of gill owing to water-borne exposure could impede the swimming activity of shrimp (Bergami et al., 2016). Second, MPs accumulation in the digestive system could reduce feeding and nutrient absorption, causing energy deficiency and subsequently weakened swimming activity of shrimp (Wang et al., 2020). Third, MPs accumulation on the large surface of gills may affect the microvilli activity, induce gill lesions and respiratory stress, which may further reduce energy consumption for swimming, in order to maintain physiological functions (Kim et al., 2021). Likewise, negative behavioral effects following MPs exposure were observed in studies using various aquatic animals. For example, 96-h of PS MPs exposure attenuated swimming activities (movement distance and maximum speed) and explorative activities of mysid shrimps (*Neomysis japonica*) (Wang et al., 2020). Similarly, decreased swimming speed and range were found in juvenile jacopever (*Sebastes schlegelii*) exposed to PS MPs, suggesting that PS MPs adversely affected the predatory performance and exploration competence of the fish (Yin et al., 2018). Additionally, study on crucian carp (*Carassius carassius*) showed PS nanoparticle-fed groups exhibited more shoaling behavior, explored lesser space of the aquarium and showed pronounced decrease in activity during feeding compared with controls (Mattsson et al., 2015). The above studies support the finding of the present research that PS MPs exposure has an adverse impact on the swimming performance and behavior of *L. vannamei*.

4.4. Oxidative stress and neurotoxicity induced by MPs

Superoxide dismutase provides the first cellular defense line against oxidative stress by converting superoxide radicals to hydrogen peroxide (Kim et al., 2021). The produced hydrogen peroxide can be further decomposed by CAT and GPx into nontoxic compounds, which help to eliminate the accumulated ROS and protect the cell from oxidative damage (Prokić et al., 2019). Our study revealed that MPs exposure caused significant elevations in the SOD activities of *L. vannamei*, accompanied by the increase of GPx activities (Fig. 3A, C). The increase in the SOD activities suggested the overproduction of superoxide radicals induced by MPs, which was compensated by increased GPx activities to neutralize the impact of peroxides to some extent (Kim et al., 2021). These phenomena probably indicate that the organisms start to build up a defensive strategy against increased ROS by enhancing antioxidant capacity (Suman et al., 2021). In contrast, another antioxidant enzyme, CAT, displayed a concentration-dependent decreasing trend in *L. vannamei* after MPs exposure (Fig. 3B). This was supported by the observed significant inverse correlation between SOD and CAT activities (Table S3). The increase in the SOD activities led to the accumulation of hydrogen peroxide, which was not efficiently scavenged by CAT, thereby leading to an imbalance of the antioxidant defense system (Kim et al., 2021). The observed inhibition of CAT activities could be attributed to ROS accumulation caused by MPs action, energy consumption for oxidative stress response, or damages in the structure of the enzyme induced by ROS (Ghelichpour et al., 2019; Yu et al., 2018). Similar inverse relationship between the CAT and SOD activities was found in mitten crabs *Eriocheir sinensis* exposed to polystyrene MPs (Yu et al., 2018) and fish larvae *Cyprinus carpio var.* exposed to polyvinyl chloride MPs (Xia et al., 2020). Moreover, the toxic product of lipid peroxidation (i.e., MDA) showed a concentration-dependent increasing trend in *L. vannamei* following MPs exposure (Fig. 3D). Hence, we interpret that the organism was unable to handle the oxidative stress caused by MPs exposure, thereafter cellular oxidative damage occurred due to lipid peroxidation (Hariharan et al., 2022; Prokić et al., 2019). AChE activity is unusually used as biomarker for assessing neurotoxicity (Suman et al., 2021). Our study did not observe the inhibition of AchE activities in the *L. vannamei* following MPs exposure, thus the observed behavioral changes of MPs-exposed organisms might be linked to other direct or indirect factors responsible for potential neurotoxic effects, such as the percentage of brain in body, the water content and morphological changes in brain (Mattsson et al., 2015; Yin et al., 2019), as well as metabolic alterations (Deng et al., 2017). Furthermore, we found that several biomarkers including SOD, CAT and MDA were significantly linked with swimming performance parameters, indicating the swimming activity and behavior were negatively affected by MPs-induced cellular oxidative stress and lipid peroxidation.

4.5. Histological alterations in the hepatopancreas induced by MPs

As demonstrated above, the hepatopancreas of *L. vannamei* was shown to accumulate most MPs of all the organs studied; as a result, the histopathological changes were particularly evident in this organ, such as tubular atrophy, loose arrangement of tubules, loss of the star-shaped lumen structure, and epithelial cell cytolysis. The degree of pathological damage was exacerbated with increasing MPs concentration (Table 1). Previous studies have also documented significant histopathological damages in the hepatopancreas, livers or digestive glands of various aquatic animals induced by MPs exposure. For instance, intramuscular administration of polyethylene MPs caused deformation and rupture of the lumen and loss of intercellular basement membrane in hepatopancreas of *L. vannamei* (Hsieh et al., 2021). Hepatopancreatic inflammation in crayfish (*Procambarus clarkii*) was observed following dietary exposure of polyethylene MPs (Zhang et al., 2022). Hepatic inflammatory responses were also revealed in the hepatocytes of PS MPs-exposed zebra fish (*Danio rerio*) (Lu et al., 2016). In addition, polyethylene and polyethylene terephthalate MPs exposure caused evident morphological abnormalities in the digestive glands of oysters (*Crassostrea gigas*), including cytoplasmic damage dispersion and necrosis (Teng et al., 2021). These histological abnormalities could be linked to oxidative stress induced by MPs, which impairs lipids, proteins, and DNA,

promotes necrosis and apoptosis in hepatocytes, and intensifies the inflammatory response (Kang et al., 2021; Sánchez-Valle et al., 2012). Moreover, it is worth noting that the hepatopancreas of crustaceans plays key roles in nutrient resorption and digestive enzyme synthesis. Thus, the severe histopathological alterations may negatively impact the normal physiological function and metabolic process of the organism.

4.6. Metabolic changes in the hepatopancreas induced by MPs

Metabolomics provides a powerful means to screen sensitive molecular biomarkers of toxicity, to identify the disturbed metabolic pathways, as well as to reveal the underlying toxicity mechanism (Bhagat et al., 2022). To further reveal the toxicity mechanism of MPs from the molecular metabolic aspects, metabolomics was performed to characterize the metabolic responses in the hepatopancreas of *L. vannamei* to MPs exposure. The statistical analyses suggested the downregulation of glyceraldehyde in the hepatopancreas induced by MPs. Glyceraldehyde is generated by the breakdown of carbohydrate, which plays key roles in connecting several metabolic pathways, particularly carbohydrate metabolism. The downregulation of glyceraldehyde might be attributed to the increased consumption of carbohydrates of *L. vannamei* to enhance the energy needs against MPs exposure conditions, consistent with the previous studies reporting the metabolism disorder of hepatic carbohydrate in zebrafish (*Danio rerio*) following MPs exposure (Sheng et al., 2021; Zhao et al., 2020).

The present research also revealed that MPs induced changes in the levels of metabolites linked to lipid metabolism, such as fatty acids and acylcarnitines in the hepatopancreas of *L. vannamei*. Free fatty acids are produced from the lipolysis process, which are then transported into mitochondria for β-oxidation by acylcarnitines, thereby releasing energy for cell activities (McCoin et al., 2015). Alterations of these metabolites indicate that MPs may disturb lipid metabolism in the hepatopancreas of *L. vannamei*. Similarly, changes of metabolites related to lipid metabolism have been demonstrated in MPs-exposed shrimp (*L. vannamei*), zebrafish (*Danio rerio*) and oyster (*Crassostrea gigas*) (Duan et al., 2021; Lu et al., 2016; Teng et al., 2021). Hepatic lipid metabolism is critical for nutrition absorption and energy production. Thus, the observed lipid metabolism abnormalities in the current study most likely indicate that MPs exposure caused a shift in the energy metabolism strategy of *L. vannamei*, which help to improve the organism's ability to handle stress. It was demonstrated that in order to satisfy the rising energy needs in stressful conditions, such as MPs exposure, organisms could adapt by presenting energetic trade-offs between various behavioral and physiological activities (Sussarellu et al., 2016). This phenomenon was also shown in marine medaka (*Oryzias melastigma*) and oyster (*Crassostrea gigas*) following MPs exposure (Feng et al., 2021; Teng et al., 2021).

Furthermore, the current study observed that MPs significantly upregulated the levels of several amino acids and dipeptides in the hepatopancreas of *L. vannamei*, indicating a disruption in amino acid metabolism. This phenomenon has also been shown in the shrimp (*L. vannamei*), zebrafish (*Danio rerio*) and oyster (*Crassostrea gigas*) exposed to MPs (Duan et al., 2021; Qiao et al., 2019; Teng et al., 2021). Amino acid metabolites can not only regulate energy metabolism, but also impact immune system function. Taurine, an abundant free intracellular amino acid present in almost all animal tissues, is actively involved in many biological and physiological functions (Surai et al., 2021). Many studies have frequently revealed that taurine can act as a protective agent against the harmful impacts of oxidative stress caused by toxic substances (Naddafi et al., 2022; Surai et al., 2021). The pronounced upregulation of hepatic taurine in *L. vannamei* after MPs exposure may reflect an attempt of the organism to enhance the antioxidant capacity of cells in order to cope with the stress conditions. L-aspartic acid, another important amino acid, functions as an intermediate of the tricarboxylic acid (TCA) cycle and the urea cycle and plays multiple roles in leukocyte metabolism and function (Gong et al., 2020). It has been reported that L-aspartic acid could relieve oxidative damage and inflammatory response in the hepatopancreas, thereby boosting fish immunity and improving survival against the bacterial infection via nitric oxide-induced phagocytosis (Gong et al., 2020; Zhao et al., 2022). Accordingly, our study found that MPs exposure caused the increased production of L-aspartic acid in *L. vannamei*, probably implying the promotion of organisms' immune responses against exogenous stressors. In addition, taurine and L-aspartic acid also act as neurotransmitters, thus the upregulation of these two metabolites might imply the potential neurotoxic effects linked to the observed behavioral changes in *L. vannamei* following MPs exposure (Deng et al., 2017). In summary, the metabolomic study demonstrated that MPs exposure could disturb glycolysis, lipolysis and amino acid metabolism pathways in the hepatopancreas of *L. vannamei*.

5. Conclusions

We characterized the toxic effects of MPs accumulation in *L. vannamei* from the aspects of behavior, tissue histology, enzyme activity and metabolome. The accumulation and distribution of MPs were demonstrated in multiple organs, with the hepatopancreas containing the most MPs. MPs accumulation caused a variety of sub-lethal effects in *L. vannamei*, including growth inhibition, swimming behavior changes, oxidative stress, and hepatopancreatic damage. Moreover, metabolomic analysis revealed that MPs interfered with hepatopancreatic metabolism of *L. vannamei* even at very low exposure level (0.02 mg L^{-1}), which offered a new perspective to delineate the toxic modes of action of MPs. Our study provides reference data for future evaluation of the harmful impact of MPs on crustaceans, which have remarkable implications for advancing our knowledge of toxic mechanisms of MPs on crustaceans. The results further highlight the potential ecological risk of MPs pollution on the populations and ecological function of marine crustaceans.

CRediT authorship contribution statement

Yingxu Zeng: Writing – original draft, Writing – review & editing, Data curation, Formal analysis, Investigation, Methodology, Visualization, Funding acquisition. **Baichuan Deng:** Data curation, Investigation, Resources, Visualization, Writing – review & editing. **Zixin Kang:** Formal analysis, Investigation. **Pedro Araujo:** Resources, Writing – review & editing. **Svein Are Mjøs:** Validation, Writing – review & editing. **Ruina Liu:** Investigation, Resources. **Jianhui Lin:** Investigation. **Tao Yang:** Investigation. **Yuangao Qu:** Formal analysis, Resources.

Declaration of Competing Interest

The authors declare that they have no known competing financial interests or personal relationships that could have appeared to influence the work reported in this paper.

Data availability

Data will be made available on request.

Acknowledgments

This work was supported by the National Natural Science Foundation of China (42167034), Hainan Provincial Natural Science Foundation of China (420RC658), Funding Scheme for High-level Overseas Chinese Students' Return of Ministry of Human Resources and Social Security of China, Science and Technology Project of Yazhou Bay Innovation Institute of Hainan Tropical Ocean University (2022CXYZD002), Hainan Provincial Joint Project of Sanya Yazhou Bay Science and Technology City (2021CXLH0009) and Scientific Research Foundation of Hainan Tropical Ocean University (RHDRC201906, RHDRC202201). The authors are grateful to the Laboratory of Extraterrestrial Ocean Systems in

the Institute of Deep-sea Science and Engneering, CAS for technical supports and the Hainan Zhongzheng Aquatic Products Technology Co., Ltd for donating the *Litopenaeus vannamei*. The authors also thank Jiangying Wu, Caijin Li and Zichuang Li for their assistance in culturing the *Litopenaeus vannamei*.

Appendix A. Supplementary material

Supplementary data associated with this article can be found in the online version at doi:10.1016/j.ecoenv.2023.114871.

References

Alimba, C.G., Faggio, C., 2019. Microplastics in the marine environment: current trends in environmental pollution and mechanisms of toxicological profile. Environ. Toxicol. Pharmacol. 68, 61–74.
Alimi, O.S., Farner Budarz, J., Hernandez, L.M., Tufenkji, N., 2018. Microplastics and nanoplastics in aquatic environments: aggregation, deposition, and enhanced contaminant transport. Environ. Sci. Technol. 52 (4), 1704–1724.
Barbosa, F., Adeyemi, J.A., Bocato, M.Z., Comas, A., Campiglia, A., 2020. A critical viewpoint on current issues, limitations, and future research needs on micro- and nanoplastic studies: from the detection to the toxicological assessment. Environ. Res. 182, 109089.
Bergami, E., Bocci, E., Vannuccini, M.L., Monopoli, M., Salvati, A., Dawson, K.A., Corsi, I., 2016. Nano-sized polystyrene affects feeding, behavior and physiology of brine shrimp *Artemia franciscana* larvae. Ecotoxicol. Environ. Saf. 123, 18–25.
Bergami, E., Pugnalini, S., Vannuccini, M., Manfra, L., Faleri, C., Savorelli, F., Dawson, K., Corsi, I., 2017. Long-term toxicity of surface-charged polystyrene nanoplastics to marine planktonic species *Dunaliella tertiolecta* and *Artemia franciscana*. Aquat. Toxicol. 189, 159–169.
Betancourt-Lozano, M., Baird, D.J., Sangha, R.S., González-Farias, F., 2006. Induction of morphological deformities and moulting alterations in *Litopenaeus vannamei* (boone) juveniles exposed to the triazole-derivative fungicide tilt. Arch. Environ. Contam. Toxicol. 51 (1), 69–78.
Bhagat, J., Zang, L., Nishimura, N., Shimada, Y., 2022. Application of omics approaches for assessing microplastic and nanoplastic toxicity in fish and seafood species. Trends Anal. Chem. 152, 116674.
Borrelle, S.B., Ringma, J., Law, K.L., Monnahan, C.C., Lebreton, L., McGivern, A., Murphy, E., Jambeck, J., Leonard, G.H., Hilleary, M.A., 2020. Predicted growth in plastic waste exceeds efforts to mitigate plastic pollution. Science 369 (6510), 1515–1518.
Cai, M., He, H., Liu, M., Li, S., Tang, G., Wang, W., Huang, P., Wei, G., Lin, Y., Chen, B., Hu, J., Cen, Z., 2018. Lost but can't be neglected: Huge quantities of small microplastics hide in the South China Sea. Sci. Total Environ. 633, 1206–1216.
Claessens, M., Meester, S.D., Landuyt, L.V., Clerck, K.D., Janssen, C.R., 2011. Occurrence and distribution of microplastics in marine sediments along the Belgian coast. Mar. Pollut. Bull. 62 (10), 2199–2204.
Cole, M., Lindeque, P., Fileman, E., Halsband, C., Galloway, T.S., 2015. The impact of polystyrene microplastics on feeding, function and fecundity in the marine copepod *Calanus helgolandicus*. Environ. Sci. Technol. 49 (2), 1130–1137.
Corteel, M., Dantas-Lima, J.J., Wille, M., Alday-Sanz, V., Pensaert, M.B., Sorgeloos, P., Nauwynck, H.J., 2012. Moult cycle of laboratory-raised *Penaeus* (*Litopenaeus*) *vannamei* and *P. monodon*. Aquac. Int. 20 (1), 13–18.
Curren, E., Leaw, C.P., Lim, P.T., Leong, S.C.Y., 2020. Evidence of marine microplastics in commercially harvested seafood. Front. Bioeng. Biotechnol. 8, 1–9.
Dawson, A.L., Kawaguchi, S., King, C.K., Townsend, K.A., King, R., Huston, W.M., Bengtson Nash, S.M., 2018. Turning microplastics into nanoplastics through digestive fragmentation by Antarctic krill. Nat. Commun. 9 (1), 1–8.
D'Costa, A.H., 2022. Microplastics in decapod crustaceans: accumulation, toxicity and impacts, a review. Sci. Total Environ. 832, 154963.
Dehaut, A., Cassone, A.-L., Frère, L., Hermabessiere, L., Himber, C., Rinnert, E., Rivière, G., Lambert, C., Soudant, P., Huvet, A., Duflos, G., Paul-Pont, I., 2016. Microplastics in seafood: Benchmark protocol for their extraction and characterization. Environ. Pollut. 215, 223–233.
Deng, Y., Zhang, Y., Lemos, B., Ren, H., 2017. Tissue accumulation of microplastics in mice and biomarker responses suggest widespread health risks of exposure. Sci. Rep. 7 (1), 46687.
Duan, Y., Xiong, D., Wang, Y., Zhang, Z., Li, H., Dong, H., Zhang, J., 2021. Toxicological effects of microplastics in *Litopenaeus vannamei* as indicated by an integrated microbiome, proteomic and metabolomic approach. Sci. Total Environ. 761, 143311.
FAO, 2022. The State of World Fisheries and Aquaculture 2022, Towards Blue Transformation. FAO, Rome.
Feng, S., Zeng, Y., Cai, Z., Wu, J., Chan, L.L., Zhu, J., Zhou, J., 2021. Polystyrene microplastics alter the intestinal microbiota function and the hepatic metabolism status in marine medaka (*Oryzias melastigma*). Sci. Total Environ. 759, 143558.
Fu, D., Chen, C.M., Qi, H., Fan, Z., Wang, Z., Peng, L., Li, B., 2020. Occurrences and distribution of microplastic pollution and the control measures in China. Mar. Pollut. Bull. 153, 110963.
Fu, J., Shen, M., Shen, Y., Lü, W., Huang, M., Luo, X., Yu, J., Ke, C., You, W., 2018. LC–MS/MS-based metabolome analysis of biochemical pathways altered by food limitation in larvae of ivory shell, *Babylonia areolata*. Mar. Biotechnol. 20 (4), 451–466.
Gambardella, C., Morgana, S., Ferrando, S., Bramini, M., Piazza, V., Costa, E., Garaventa, F., Faimali, M., 2017. Effects of polystyrene microbeads in marine planktonic crustaceans. Ecotoxicol. Environ. Saf. 145, 250–257.
Ghelichpour, M., Taheri Mirghaed, A., Hoseinifar, S.H., Khalili, M., Yousefi, M., Van Doan, H., Perez-Jimenez, A., 2019. Expression of immune, antioxidant and stress related genes in different organs of common carp exposed to indoxacarb. Aquat. Toxicol. 208, 208–216.
Gong, Q., Yang, D., Jiang, M., Zheng, J., Peng, B., 2020. L-aspartic acid promotes fish survival against Vibrio alginolyticus infection through nitric oxide-induced phagocytosis. Fish. Shellfish Immunol. 97, 359–366.
Hara, J., Frias, J., Nash, R., 2020. Quantification of microplastic ingestion by the decapod crustacean *Nephrops norvegicus* from Irish waters. Mar. Pollut. Bull. 152, 110905.
Hariharan, G., Purvaja, R., Anandavelu, I., Robin, R., Ramesh, R., 2022. Ingestion and toxic impacts of weathered polyethylene (wPE) microplastics and stress defensive responses in whiteleg shrimp (*Penaeus vannamei*). Chemosphere 300, 134487.
Hsieh, S.-L., Wu, Y.-C., Xu, R.-Q., Chen, Y.-T., Chen, C.-W., Singhania, R.R., Dong, C.-D., 2021. Effect of polyethylene microplastics on oxidative stress and histopathology damages in *Litopenaeus vannamei*. Environ. Pollut. 288, 117800.
Jeong, C.-B., Won, E.-J., Kang, H.-M., Lee, M.-C., Hwang, D.-S., Hwang, U.-K., Zhou, B., Souissi, S., Lee, S.-J., Lee, J.-S., 2016. Microplastic size-dependent toxicity, oxidative stress induction, and p-JNK and p-p38 activation in the monogonont rotifer (*Brachionus koreanus*). Environ. Sci. Technol. 50 (16), 8849–8857.
Kane, I.A., Clare, M.A., Miramontes, E., Wogelius, R., Rothwell, J.J., Garreau, P., Pohl, F., 2020. Seafloor microplastic hotspots controlled by deep-sea circulation. Science 368 (6495), 1140–1145.
Kang, H.-M., Byeon, E., Jeong, H., Kim, M.-S., Chen, Q., Lee, J.-S., 2021. Different effects of nano-and microplastics on oxidative status and gut microbiota in the marine medaka *Oryzias melastigma*. J. Hazard. Mater. 405, 124207.
Kang, J.-H., Kwon, O.Y., Lee, K.-W., Song, Y.K., Shim, W.J., 2015. Marine neustonic microplastics around the southeastern coast of Korea. Mar. Pollut. Bull. 96 (1), 304–312.
Kim, J.-H., Yu, Y.-B., Choi, J.-H., 2021. Toxic effects on bioaccumulation, hematological parameters, oxidative stress, immune responses and neurotoxicity in fish exposed to microplastics: a review. J. Hazard. Mater. 413, 125423.
Kögel, T., Bjorøy, Ø., Toto, B., Bienfait, A.M., Sanden, M., 2020. Micro-and nanoplastic toxicity on aquatic life: determining factors. Sci. Total Environ. 709, 136050.
Kolandhasamy, P., Su, L., Li, J., Qu, X., Jabeen, K., Shi, H., 2018. Adherence of microplastics to soft tissue of mussels: a novel way to uptake microplastics beyond ingestion. Sci. Total Environ. 610–611, 635–640.
Lee, K.-W., Shim, W.J., Kwon, O.Y., Kang, J.-H., 2013. Size-dependent effects of micro polystyrene particles in the marine copepod *Tigriopus japonicus*. Environ. Sci. Technol. 47 (19), 11278–11283.
Lenz, R., Enders, K., Nielsen, T.G., 2016. Microplastic exposure studies should be environmentally realistic. Proc. Natl. Acad. Sci. 113 (29), e4121–e4122.
Li, R., Zhang, S., Zhang, L., Yu, K., Wang, S., Wang, Y., 2020a. Field study of the microplastic pollution in sea snails (*Ellobium chinense*) from mangrove forest and their relationships with microplastics in water/sediment located on the north of Beibu Gulf. Environ. Pollut. 263, 114368.
Li, Z., Feng, C., Wu, Y., Guo, X., 2020b. Impacts of nanoplastics on bivalve: fluorescence tracing of organ accumulation, oxidative stress and damage. J. Hazard. Mater. 392, 122418.
Lin, W., Luo, H., Wu, J., Liu, X., Cao, B., Hung, T.-C., Liu, Y., Chen, Z., Yang, P., 2022. Distinct vulnerability to oxidative stress determines the ammonia sensitivity of crayfish (*Procambarus clarkii*) at different developmental stages. Ecotoxicol. Environ. Saf. 242, 113895.
Lu, Y., Zhang, Y., Deng, Y., Jiang, W., Zhao, Y., Geng, J., Ding, L., Ren, H., 2016. Uptake and accumulation of polystyrene microplastics in zebrafish (*Danio rerio*) and toxic effects in liver. Environ. Sci. Technol. 50 (7), 4054–4060.
Mattsson, K., Ekvall, M.T., Hansson, L.-A., Linse, S., Malmendal, A., Cedervall, T., 2015. Altered behavior, physiology, and metabolism in fish exposed to polystyrene nanoparticles. Environ. Sci. Technol. 49 (1), 553–561.
McCoin, C.S., Knotts, T.A., Adams, S.H., 2015. Acylcarnitines—old actors auditioning for new roles in metabolic physiology. Nat. Rev. Endocrinol. 11 (10), 617–625.
Mkuye, R., Gong, S., Zhao, L., Masanja, F., Ndandala, C., Bubelwa, E., Yang, C., Deng, Y., 2022. Effects of microplastics on physiological performance of marine bivalves, potential impacts, and enlightening the future based on a comparative study. Sci. Total Environ. 838, 155933.
Naddafi, M., Eghbal, M.A., Khansari, M.G., Sattari, M.R., Azarmi, Y., Samadi, M., Mehrizi, A.A., 2022. Sensing of oxidative stress biomarkers: the cardioprotective effect of taurine & grape seed extract against the poisoning induced by an agricultural pesticide aluminum phosphide. Chemosphere 287, 132245.
Phuong, N.N., Zalouk-Vergnoux, A., Poirier, L., Kamari, A., Châtel, A., Mouneyrac, C., Lagarde, F., 2016. Is there any consistency between the microplastics found in the field and those used in laboratory experiments? Environ. Pollut. 211, 111–123.
Prokić, M.D., Radovanović, T.B., Gavrić, J.P., Faggio, C., 2019. Ecotoxicological effects of microplastics: examination of biomarkers, current state and future perspectives. Trends Anal. Chem. 111, 37–46.
Qiao, R., Sheng, C., Lu, Y., Zhang, Y., Ren, H., Lemos, B., 2019. Microplastics induce intestinal inflammation, oxidative stress, and disorders of metabolome and microbiome in zebrafish. Sci. Total Environ. 662, 246–253.
Rodriguez, A., Zhang, H., Klaminder, J., Brodin, T., Andersson, P.L., Andersson, M., 2018. ToxTrac: a fast and robust software for tracking organisms. Methods Ecol. Evol. 9 (3), 460–464.

Saborowski, R., Korez, Š., Riesbeck, S., Weidung, M., Bickmeyer, U., Gutow, L., 2022. Shrimp and microplastics: a case study with the Atlantic ditch shrimp *Palaemon varians*. Ecotoxicol. Environ. Saf. 234, 113394.

Sánchez-Valle, V., C Chavez-Tapia, N., Uribe, M., Méndez-Sánchez, N., 2012. Role of oxidative stress and molecular changes in liver fibrosis: a review. Curr. Med. Chem. 19 (28), 4850–4860.

Sheng, C., Zhang, S., Zhang, Y., 2021. The influence of different polymer types of microplastics on adsorption, accumulation, and toxicity of triclosan in zebrafish. J. Hazard. Mater. 402, 123733.

Sousa, L., Petriella, A.M., 2006. Morphology and histology of *P. argentinus* (Crustacea, Decapoda, Caridea) digestive tract. Biocell 30 (2), 287–294.

Suman, K.H., Haque, M.N., Uddin, M.J., Begum, M.S., Sikder, M.H., 2021. Toxicity and biomarkers of micro-plastic in aquatic environment: a review. Biomarkers 26 (1), 13–25.

Surai, P.F., Earle-Payne, K., Kidd, M.T., 2021. Taurine as a natural antioxidant: from direct antioxidant effects to protective action in various toxicological models. Antioxidants 10 (12), 1876.

Sussarellu, R., Suquet, M., Thomas, Y., Lambert, C., Fabioux, C., Pernet, M.E.J., Le Goïc, N., Quillien, V., Mingant, C., Epelboin, Y., 2016. Oyster reproduction is affected by exposure to polystyrene microplastics. Proc. Natl. Acad. Sci. 113 (9), 2430–2435.

Teng, J., Zhao, J., Zhu, X., Shan, E., Zhang, C., Zhang, W., Wang, Q., 2021. Toxic effects of exposure to microplastics with environmentally relevant shapes and concentrations: accumulation, energy metabolism and tissue damage in oyster *Crassostrea gigas*. Environ. Pollut. 269, 116169.

Valencia-Castañeda, G., Ibáñez-Aguirre, K., Rebolledo, U.A., Capparelli, M.V., Páez-Osuna, F., 2022a. Microplastic contamination in wild shrimp *Litopenaeus vannamei* from the Huizache-Caimanero Coastal lagoon, SE Gulf of California. Bull. Environ. Contam. Toxicol. 109 (3), 425–430.

Valencia-Castañeda, G., Ruiz-Fernández, A.C., Frías-Espericueta, M.G., Rivera-Hernández, J.R., Green-Ruiz, C.R., Páez-Osuna, F., 2022b. Microplastics in the tissues of commercial semi-intensive shrimp pond-farmed *Litopenaeus vannamei* from the Gulf of California ecoregion. Chemosphere 297, 134194.

Von Moos, N., Burkhardt-Holm, P., Köhler, A., 2012. Uptake and effects of microplastics on cells and tissue of the blue mussel *Mytilus edulis L.* after an experimental exposure. Environ. Sci. Technol. 46 (20), 11327–11335.

Wang, S., Hu, M., Zheng, J., Huang, W., Shang, Y., Fang, J.K.-H., Shi, H., Wang, Y., 2021a. Ingestion of nano/micro plastic particles by the mussel *Mytilus coruscus* is size dependent. Chemosphere 263, 127957.

Wang, Z., Fan, L., Wang, J., Xie, S., Zhang, C., Zhou, J., Zhang, L., Xu, G., Zou, J., 2021b. Insight into the immune and microbial response of the white-leg shrimp *Litopenaeus vannamei* to microplastics. Mar. Environ. Res. 169, 105377.

Wang, X., Liu, L., Zheng, H., Wang, M., Fu, Y., Luo, X., Li, F., Wang, Z., 2020. Polystyrene microplastics impaired the feeding and swimming behavior of mysid shrimp *Neomysis japonica*. Mar. Pollut. Bull. 150, 110660.

Watts, A.J., Urbina, M.A., Corr, S., Lewis, C., Galloway, T.S., 2015. Ingestion of plastic microfibers by the crab *Carcinus maenas* and its effect on food consumption and energy balance. Environ. Sci. Technol. 49 (24), 14597–14604.

Wegner, A., Besseling, E., Foekema, E.M., Kamermans, P., Koelmans, A.A., 2012. Effects of nanopolystyrene on the feeding behavior of the blue mussel (*Mytilus edulis L.*). Environ. Toxicol. Chem. 31 (11), 2490–2497.

Xia, X., Sun, M., Zhou, M., Chang, Z., Li, L., 2020. Polyvinyl chloride microplastics induce growth inhibition and oxidative stress in *Cyprinus carpio* var. larvae. Sci. Total Environ. 716, 136479.

Yin, L., Chen, B., Xia, B., Shi, X., Qu, K., 2018. Polystyrene microplastics alter the behavior, energy reserve and nutritional composition of marine jacopever (*Sebastes schlegelii*). J. Hazard. Mater. 360, 97–105.

Yin, L., Liu, H., Cui, H., Chen, B., Li, L., Wu, F., 2019. Impacts of polystyrene microplastics on the behavior and metabolism in a marine demersal teleost, black rockfish (*Sebastes schlegelii*). J. Hazard. Mater. 380, 120861.

Yu, P., Liu, Z., Wu, D., Chen, M., Lv, W., Zhao, Y., 2018. Accumulation of polystyrene microplastics in juvenile *Eriocheir sinensis* and oxidative stress effects in the liver. Aquat. Toxicol. 200, 28–36.

Zhang, X., Jin, Z., Shen, M., Chang, Z., Yu, G., Wang, L., Xia, X., 2022. Accumulation of polyethylene microplastics induces oxidative stress, microbiome dysbiosis and immunoregulation in crayfish. Fish. Shellfish Immunol. 125, 276–284.

Zhao, X., Yang, Y., Wang, L., Chen, H., Zhu, L., Li, L., Kong, X., 2022. Aspartate induces metabolic changes and improves the host's ability to fight against Aeromonas hydrophila infection in *Cyprinus carpio*. Aquac. Res. 53 (3), 1050–1061.

Zhao, Y., Bao, Z., Wan, Z., Fu, Z., Jin, Y., 2020. Polystyrene microplastic exposure disturbs hepatic glycolipid metabolism at the physiological, biochemical, and transcriptomic levels in adult zebrafish. Sci. Total Environ. 710, 136279.

Zitouni, N., Bousserrhine, N., Missawi, O., Boughattas, I., Chèvre, N., Santos, R., Belbekhouche, S., Alphonse, V., Tisserand, F., Balmassiere, L., 2021. Uptake, tissue distribution and toxicological effects of environmental microplastics in early juvenile fish *Dicentrarchus labrax*. J. Hazard. Mater. 403, 124055.